Low energy pion-hyperon interaction

C. C. Barros, Jr. and Y. Hama
Instituto de Física, Universidade de São Paulo, C.P. 66318, 05315-970 São Paulo-SP, Brazil
(Received 22 December 2000; published 18 May 2001)

We study the low energy pion-hyperon interaction considering effective nonlinear chiral invariant Lagrangians including pions, ρ mesons, σ mesons, hyperons, and corresponding resonances. Then we calculate the *S*- and *P*-wave phase shifts, total cross sections, angular distributions, and polarizations for the momentum in the center-of-mass frame up to $k=400$ MeV. With these results we discuss the *CP* violation in the $\Xi \rightarrow \Lambda\pi$ and $\Omega \rightarrow \Xi\pi$ weak decays.

DOI: 10.1103/PhysRevC.63.065203 PACS number(s): 13.75.Gx, 13.88.+e

I. INTRODUCTION

Why should we study pion-hyperon (πY) interaction? It is not hard to see that, due to their instability, it is not an easy task for an experimentalist to make beams of pions and hyperons, let them collide and study what happens in such collisions. As far as we know, no experimental data on the πY interaction are available. In such a situation, is there any practical interest, besides an academic one, in theoretically studying these interactions?

In 1957, Okubo [1] observed that the *CP* violation allows Σ and $\overline{\Sigma}$ to have different branching ratios into conjugate channels. Pais [2] extended this proposal also to Λ and $\overline{\Lambda}$ decays. In these reactions, the final-state strong interaction between the decay products plays a very important role. The few studies on πY interactions we could find in the literature [3–5] are related to the $\Xi \rightarrow \pi\Lambda$ decay, in which an independent estimate of the $\pi\Lambda$ strong phase shifts is needed to correctly analyze the data and conclude about the *CP* violation. In these references, however, the results presented show some discrepancy among them, especially on δ_S, requiring a clarification. As for the other interactions, such as $\pi\Sigma$ and $\pi\Xi$, within our limited knowledge no study has ever been done.

Besides, we have a somewhat different motivation for the present study. It is by now well known that in high-energy proton-nucleus collisions, the inclusively produced hyperons appear usually polarized [6–8]. Several models have been proposed to explain this phenomenon [9–13], which at least qualitatively, or even quantitatively, can account for the *hyperon* polarization. However, as for the *antihyperons* which are generally produced also with polarization [7,8], these models are not applicable, since all of them are based on some leading-particle effect in which the incident proton is transformed into a leading hyperon.[1] In [15], it is proposed that at least part of the polarization is caused by the final-state interaction of (anti-)hyperon with the surrounding hot medium where it is produced during the collision of the incident objects. This mechanism would be the dominant one in the case of antihyperon polarization, since they cannot be produced as leading particles. In [15], this idea was put forward within a hydrodynamic model, by treating the interaction with the hot medium as given by an optical potential, reproducing all the qualitative features of the existing data. Evidently, it is desirable that, if possible, more realistic microscopic interaction be used instead of purely phenomenological potential with fitted parameters. Since pions are dominant in such a hot medium mentioned above, the microscopic interactions of our interest would be pion-hyperon (or more precisely pion-antihyperon) interactions. However, except for few results on $\pi\Lambda$, we are not aware of any study on these interactions. So the main object of the present work is to study the low-energy (with respect to the surrounding medium) pion-hyperon interactions, aiming at a later computation of antihyperon polarization in high-energy hadron-nucleus collisions.

The plan of presentation is the following. We shall first explain, in the next section, the general strategy of treating the pion-hyperon interactions. Then, in Secs. III, IV, and V, we apply it, respectively, to the $\pi-\Lambda$, $\pi-\Sigma$, and $\pi-\Xi$ cases. Phase shifts are calculated and from these the energy dependence of the total cross section, the angular distribution and the polarization for each reaction are computed in these sections. Conclusions are drawn in Sec. VI. The basic formalism is given in the Appendix.

II. STRATEGY FOR THE STUDY OF THE PION-HYPERON INTERACTIONS

How could we proceed to study the low-energy $\pi\overline{Y}$ interactions? First of all, due to the *CPT* invariance, it is enough to study the πY interactions instead of the $\pi\overline{Y}$ ones. For instance, the $\overline{Y}$ polarization is obtained from the corresponding one for *Y*, just by changing the sign. Next, recall that unlike the πY ones, the low-energy πN interaction is, for obvious reasons, very well studied for a long time. There is a large amount of experimental data, and also many models [16–21] that reproduce them pretty well. Here, we shall consider a chiral-invariant effective Lagrangian model. In [22], such a Lagrangian was written in terms of π, *N*, ρ and Δ fields as a sum of

$$\mathcal{L}_{N\pi N}=\frac{g}{2m}[\overline{N}\gamma_\mu\gamma_5\vec{\tau}N]\partial^\mu\vec{\phi}, \tag{1}$$

[1]It should be mentioned that in a recent paper [14], a parametrization of Λ and $\overline{\Lambda}$ polarization data has been carried out in terms of polarizing fragmentation functions.

$$\mathcal{L}_{N\pi\Delta}=g_\Delta\left\{\overline{\Delta}^\mu\left[g_{\mu\nu}-\left(Z+\frac{1}{2}\right)\gamma_\mu\gamma_\nu\right]\vec{M}N\right\}\partial^\nu\vec{\phi}+\text{H.c.}, \tag{2}$$

$$\mathcal{L}_{N\rho N}=\frac{g_0}{2}[\overline{N}\gamma_\mu\vec{\tau}N]\vec{\rho}^\mu+\frac{g_0}{2}\left[\overline{N}\left(\frac{\mu_p-\mu_n}{4m}\right)i\sigma_{\mu\nu}\vec{\tau}N\right]\times(\partial^\mu\vec{\rho}^\nu-\partial^\nu\vec{\rho}^\mu), \tag{3}$$

$$\mathcal{L}_{\pi\rho\pi}=g_0\vec{\rho}_\mu(\vec{\phi}\times\partial^\mu\vec{\phi})-\frac{g_0}{4m_\rho^2}(\partial_\mu\vec{\rho}_\nu-\partial_\nu\vec{\rho}_\mu)(\partial^\mu\vec{\phi}\times\partial^\nu\vec{\phi}), \tag{4}$$

where N, Δ, $\vec{\phi}$, $\vec{\rho}$ are the nucleon, delta, pion, and rho fields with masses m, m_Δ, m_π, and m_ρ, respectively, μ_p and μ_n are the proton and neutron magnetic moments, $\vec{M}$ and $\vec{\tau}$ are the isospin matrices, and Z is a parameter representing the possibility of the off-shell-Δ having spin 1/2. In addition, it also included a σ term as a correction and parametrized it in a way we will show below.

Now, since $\pi\Lambda$, $\pi\Sigma$ and $\pi\Xi$ systems are similar to πN, we can make an analogy and use the same prescription explained above, adapting it appropriately. The $\Delta(1232)$ resonance plays a central role in the low-energy πN interaction. Its contribution dominates the total cross section of π^+p ($T=3/2$) process and is also important to the other isospin channels. The lowest energy hyperon resonances and their main decay modes are quite well known, so it is possible to use these resonances replacing $\Delta(1232)$. As for the coupling constants, they can be estimated from the resonance widths [5].

Another detail we have to take into account is the unitarization of the amplitudes. In an effective model like the one we are considering, the amplitudes we directly obtain are real, and consequently violate the unitarity of the S matrix. So, if we want something more than a simple cross section, some procedure is required to unitarize the amplitudes. As is often done in effective models [18,20,21,23], and will be explained in detail in the next section, we will do this by reinterpreting the calculated amplitudes as elements of reaction matrix K.

Now we are ready to calculate all the phase shifts and then the total cross sections, angular distributions, and polarizations. Because we are interested in low energies ($k\leqslant 0.4$ GeV), we will limit ourselves to the S and P waves, which are generally enough for our purpose.

III. PION-LAMBDA INTERACTION

The $\pi\Lambda$ interaction is the simplest case. Since Λ has isospin 0, the scattering amplitude $T_{\pi\Lambda}$ has the general form

$$T^{ba}_{\pi\Lambda}=\overline{u}(\vec{p}')\left[A(k,\theta)+\frac{(\not{k}+\not{k}')}{2}B(k,\theta)\right]\delta_{ba}u(\vec{p}), \tag{5}$$

where p_μ and p'_μ are the initial and final four-momenta of Λ in the center-of-mass frame, k_μ and k'_μ are those of the pion, and θ the scattering angle. Indices a and b indicate the initial and final isospin states of the pion. We show in Fig. 1 the relevant diagrams, where we have omitted the crossed diagrams, although included in the calculations. We consider only the first resonance $\Sigma^*(1385)$, because we are interested in the low-energy ($k\leqslant 0.4$ GeV) behavior. The ρ exchange term is absent in the $\pi\Lambda$ case, because due to the isospin it does not couple to Λ. To compute the first two of these diagrams, the Lagrangians (1) and (2) have been adapted to

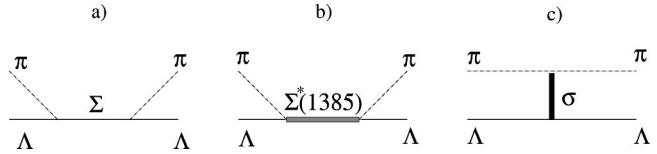

FIG. 1. Diagrams for $\pi\Lambda$ interaction.

$$\mathcal{L}_{\Lambda\pi\Sigma}=\frac{g_{\Lambda\pi\Sigma}}{2m_\Lambda}[\overline{\Sigma}_\alpha\gamma_\mu\gamma_5\Lambda]\partial^\mu\phi_\alpha+\text{H.c.}, \tag{6}$$

$$\mathcal{L}_{\Lambda\pi\Sigma*}=g_{\Lambda\pi\Sigma*}\left\{\overline{\Sigma}^{*\mu}_\alpha\left[g_{\mu\nu}-\left(Z+\frac{1}{2}\right)\gamma_\mu\gamma_\nu\right]\Lambda\right\}\partial^\nu\phi_\alpha+\text{H.c.}, \tag{7}$$

by replacing the nucleon by Λ or Σ, and Δ by Σ^* and performing appropriate sums over isotopic spin indices.

The contributions of Fig. 1(a) to the amplitudes are

$$A_\Sigma=\frac{g^2_{\Lambda\pi\Sigma}}{4m^2_\Lambda}(m_\Lambda+m_\Sigma)\left\{\frac{s-m^2_\Lambda}{s-m^2_\Sigma}+\frac{u-m^2_\Lambda}{u-m^2_\Sigma}\right\},$$

$$B_\Sigma=\frac{g^2_{\Lambda\pi\Sigma}}{4m^2_\Lambda}\left\{\frac{m^2_\Lambda-s-2m_\Lambda(m_\Lambda+m_\Sigma)}{s-m^2_\Sigma}+\frac{2m_\Lambda(m_\Lambda+m_\Sigma)+u-m^2_\Lambda}{u-m^2_\Sigma}\right\}. \tag{8}$$

Figure 1(b) gives

$$A_{\Sigma*}=\frac{g^2_{\Lambda\pi\Sigma*}}{3m_\Lambda}\left\{\frac{\nu_r}{\nu_r^2-\nu^2}\hat{A}-\frac{m^2_\Lambda+m_\Lambda m_{\Sigma*}}{m^2_{\Sigma*}}\times(2m^2_{\Sigma*}+m_\Lambda m_{\Sigma*}-m^2_\Lambda+2m^2_\pi)+\frac{4m_\Lambda}{m^2_{\Sigma*}}[(m_\Lambda+m_{\Sigma*})Z+(2m_{\Sigma*}+m_\Lambda)Z^2]k\cdot k'\right\},$$

$$B_{\Sigma*}=\frac{g^2_{\Lambda\pi\Sigma*}}{3m_\Lambda}\left\{\frac{\nu}{\nu_r^2-\nu^2}\hat{B}-\frac{8m^2_\Lambda\nu Z^2}{m^2_{\Sigma*}}\right\}, \tag{9}$$

where ν and ν_r are defined in the Appendix and

$$\hat{A}=\frac{(m_{\Sigma*}+m_\Lambda)^2-m_\pi^2}{2m_{\Sigma*}^2}[2m_{\Sigma*}^3-2m_\Lambda^3-2m_\Lambda m_{\Sigma*}^2-2m_\Lambda^2 m_{\Sigma*}+m_\pi^2(2m_\Lambda-m_{\Sigma*})]+\frac{3}{2}(m_\Lambda+m_{\Sigma*})t,$$

$$\hat{B}=\frac{1}{2m_{\Sigma*}^2}[(m_{\Sigma*}^2-m_\Lambda^2)^2-2m_\pi^2(m_{\Sigma*}+m_\Lambda)^2+m_\pi^4]+\frac{3}{2}t. \tag{10}$$

As for Fig. 1(c), we only parametrize the amplitudes as done in [16]

$$A_\sigma=a+bt,$$
$$B_\sigma=0, \tag{11}$$

where $a=1.05m_\pi^{-1}$ and $b=-0.80m_\pi^{-3}$ are constants (we use the same values of [22] for πN). The scattering matrix will then have the form

$$M_{ba}=\frac{T_{ba}}{8\pi\sqrt{s}}=f_1+\frac{(\vec{\sigma}\cdot\vec{k})(\vec{\sigma}\cdot\vec{k}')}{kk'}f_2 \tag{12}$$

and we can make the partial wave decomposition with

$$a_{l\pm}=\frac{1}{2}\int_{-1}^{1}[P_l(x)f_1(x)+P_{l\pm1}(x)f_2(x)]dx. \tag{13}$$

The amplitudes $a_{l\pm}$, calculated in a tree-level approximation, are real and, so, the corresponding S matrix is not unitary. In order to unitarize these amplitudes, we reinterpret them as elements of K matrix and write

$$a_{l\pm}^U=\frac{a_{l\pm}}{1-ika_{l\pm}}. \tag{14}$$

The phase shifts are then computed as

$$\delta_{l\pm}=\mathrm{tg}^{-1}(ka_{l\pm}). \tag{15}$$

The parameters we use are $m_\Lambda=1.115$ GeV, $m_\Sigma=1.192$ GeV, $m_{\Sigma*}=1.385$ GeV, $m_\pi=0.139$ GeV [25], $g_{\Lambda\pi\Sigma}=11.7$ [26,27] and $Z=-0.5$ [22]. The only parameter that is missing is $g_{\Lambda\pi\Sigma*}$. As mentioned before, we estimate it from the resonance width. Namely, by comparing the δ_{P3} phase shift in the resonance region with the relativistic Breit-Wigner expression [24],

$$\delta_{l\pm}=\mathrm{tg}^{-1}\left[\frac{\Gamma_0\left(\frac{k}{k_0}\right)^{2l}}{2(m_r-\sqrt{s})}\right], \tag{16}$$

where k_0 is the center-of-mass momentum at the peak of $\Sigma^*(1385)$, that is 0.207 GeV. The value obtained in this way is $g_{\Lambda\pi\Sigma*}=9.38\ \mathrm{GeV}^{-1}$, which we will use here.

In Fig. 2, we show the calculated phase-shifts as functions of the center-of-mass momentum k. We also show there the k dependence of the total elastic cross section, the angular distribution and the Λ polarization as function of $x=\cos\theta$, for $k=100$, 200, 300 and 400 MeV.

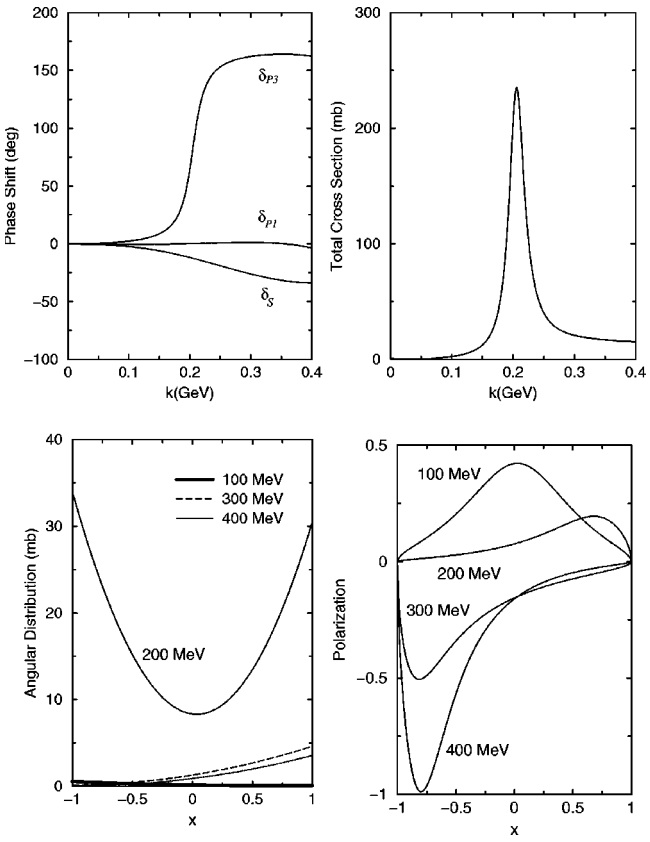

FIG. 2. $\pi\Lambda$ scattering.

As we can see, the $\Sigma^*(1385)$ contribution dominates the total elastic cross section in the low energy region (quite similar to π^+p scattering). As for the polarization, it begins positive at lower energies and then becomes negative above $k\sim k_0$.

IV. PION-SIGMA INTERACTION

In the case of $\pi\Sigma$ interaction, both π and Σ have isospin 1, so the compound system can have isospin 2, 1, or 0. For this reason, the scattering amplitude is somewhat more complex in this case and has the following general form:

$$\begin{aligned}T_{\alpha\gamma,\beta\delta}&=\langle\pi_\gamma\Sigma_\delta|T|\pi_\alpha\Sigma_\beta\rangle\\&=\bar{u}(\vec{p}')\left\{\left[A+\frac{(\not{k}+\not{k}')}{2}A'\right]\delta_{\alpha\beta}\delta_{\gamma\delta}\right.\\&\quad+\left[B+\frac{(\not{k}+\not{k}')}{2}B'\right]\delta_{\alpha\gamma}\delta_{\beta\delta}\\&\quad\left.+\left[C+\frac{(\not{k}+\not{k}')}{2}C'\right]\delta_{\alpha\delta}\delta_{\beta\gamma}\right\}u(\vec{p}),\end{aligned} \tag{17}$$

where α, β, γ and δ are isospin indices. Decomposing this amplitude into the ith. isospin states of the system (P_i are the projection operators), we have

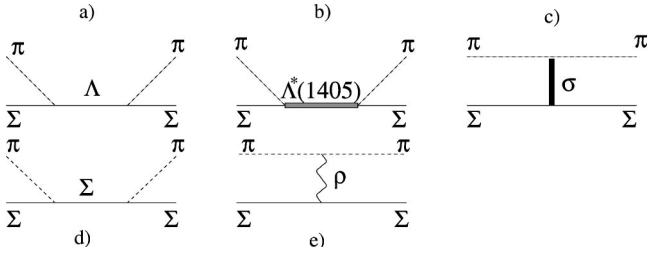

FIG. 3. Diagrams to $\pi\Sigma$ interaction.

$$
\begin{aligned}
T_{\alpha\gamma,\beta\delta} = \overline{u}(\vec{p}')\Bigg\{ & \left[A_0 + \frac{(\not{k}+\not{k}')}{2} B_0\right] P_0 \\
& + \left[A_1 + \frac{(\not{k}+\not{k}')}{2} B_1\right] P_1 \\
& + \left[A_2 + \frac{(\not{k}+\not{k}')}{2} B_2\right] P_2 \Bigg\} u(\vec{p}) \\
= \overline{u}(\vec{p}')\Bigg\{ & \frac{1}{3}\left[A_0 + \frac{(\not{k}+\not{k}')}{2} B_0\right] \delta_{\alpha\beta}\delta_{\gamma\delta} \\
& + \frac{1}{2}\left[A_1 + \frac{(\not{k}+\not{k}')}{2} B_1\right] [\delta_{\alpha\gamma}\delta_{\beta\delta} - \delta_{\alpha\delta}\delta_{\beta\gamma}] \\
& + \frac{1}{6}\left[A_2 + \frac{(\not{k}+\not{k}')}{2} B_2\right] \\
& \times [3\delta_{\alpha\gamma}\delta_{\beta\delta} + 3\delta_{\alpha\delta}\delta_{\beta\gamma} - \delta_{\alpha\beta}\delta_{\gamma\delta}] \Bigg\} u(\vec{p}). \quad (18)
\end{aligned}
$$

Comparing Eqs. (17) and (18) we obtain

$$
\begin{aligned}
A_0 &= 3A + B + C, \quad B_0 = 3A' + B' + C', \\
A_1 &= B - C, \quad B_1 = B' - C', \\
A_2 &= B + C, \quad B_2 = B' + C'.
\end{aligned} \quad (19)
$$

These are the relations that determine all the amplitudes projected on isospin states.

The interaction Lagrangians are given by Eqs. (4), (6) and

$$
\mathcal{L}_{\Sigma\pi\Sigma} = \frac{g_{\Sigma\pi\Sigma}}{2m_\Sigma} [\overline{\Sigma}\gamma_\mu\gamma_5 \vec{t}\Sigma]\partial^\mu\vec{\phi}, \quad (20)
$$

$$
\mathcal{L}_{\Sigma\rho\Sigma} = \frac{g_0}{2}[\overline{\Sigma}\gamma_\mu\vec{t}\Sigma]\vec{\rho}^\mu + \frac{g_0}{2}\left[\overline{\Sigma}\left(\frac{\mu_{\Sigma^0} - \mu_{\Sigma^-}}{4m_\Sigma}\right) i\sigma_{\mu\nu}\vec{t}\Sigma\right] (\partial^\mu\vec{\rho}^\nu - \partial^\nu\vec{\rho}^\mu), \quad (21)
$$

where the isospin combination matrix $\vec{t}$ obeys

$$
\langle\beta|\vec{t}|\alpha\rangle = -i\epsilon_{\beta\alpha c}\hat{e}_c. \quad (22)
$$

Figure 3 shows the diagrams we consider for the $\pi\Sigma$ interactions. $\Sigma^*(1385)$ also couples to $\pi\Sigma$, but its decay branching ratio back to the $\pi\Sigma$ channel is only 11%. So, we will neglect it.

The amplitudes corresponding to Fig. 3(a) are

$$
\begin{aligned}
A_\Lambda &= \frac{g^2_{\Lambda\pi\Sigma}}{4m^2_\Sigma}(m_\Sigma + m_\Lambda)\frac{s - m^2_\Sigma}{s - m^2_\Lambda}, \\
B_\Lambda &= 0, \\
C_\Lambda &= \frac{g^2_{\Lambda\pi\Sigma}}{4m^2_\Sigma}(m_\Sigma + m_\Lambda)\frac{u - m^2_\Sigma}{u - m^2_\Lambda}, \\
A'_\Lambda &= \frac{g^2_{\Lambda\pi\Sigma}}{4m^2_\Sigma}\frac{m^2_\Sigma - s - 2m_\Sigma(m_\Sigma + m_\Lambda)}{s - m^2_\Lambda}, \\
B'_\Lambda &= 0, \\
C'_\Lambda &= \frac{g^2_{\Lambda\pi\Sigma}}{4m^2_\Sigma}\frac{2m_\Sigma(m_\Sigma + m_\Lambda) + u - m^2_\Sigma}{u - m^2_\Lambda}.
\end{aligned} \quad (23)
$$

The contributions of Fig. 3(b) with intermediate $\Lambda^*(1405)$ are similar. We must only change the coupling constant and replace the mass m_Λ by m_{Λ^*}.

In the case of the intermediate Σ, Fig. 3(d), we have

$$
\begin{aligned}
A_\Sigma &= -\frac{g^2_{\Sigma\pi\Sigma}}{2m_\Sigma}, \\
B_\Sigma &= \frac{g^2_{\Sigma\pi\Sigma}}{m_\Sigma}, \\
C_\Sigma &= -\frac{g^2_{\Sigma\pi\Sigma}}{2m_\Sigma}, \\
A'_\Sigma &= -\frac{g^2_{\Sigma\pi\Sigma}}{4m^2_\Sigma} - \frac{g^2_{\Sigma\pi\Sigma}}{2m_\Sigma}\frac{1}{\nu_0 - \nu}, \\
B'_\Sigma &= \frac{g^2_{\Sigma\pi\Sigma}}{m_\Sigma}\frac{\nu}{\nu_0^2 - \nu^2}, \\
C'_\Sigma &= \frac{g^2_{\Sigma\pi\Sigma}}{4m^2_\Sigma} + \frac{g^2_{\Sigma\pi\Sigma}}{2m_\Sigma}\frac{1}{\nu_0 + \nu}.
\end{aligned} \quad (24)
$$

The ρ exchange amplitude, Fig. 3(e), has the form

$$
T_\rho = \overline{u}(\vec{p}')\left[A_\rho + \frac{(\not{k}+\not{k}')}{2} B_\rho\right][\delta_{\alpha\beta}\delta_{\gamma\delta} - \delta_{\alpha\delta}\delta_{\beta\gamma}]u(\vec{p}), \quad (25)
$$

so

$$
\begin{aligned}
A_0 &= 2A_\rho, \quad B_0 = 2B_\rho, \\
A_1 &= A_\rho, \quad B_1 = B_\rho, \\
A_2 &= -A_\rho, \quad B_2 = -B_\rho,
\end{aligned} \quad (26)
$$

with

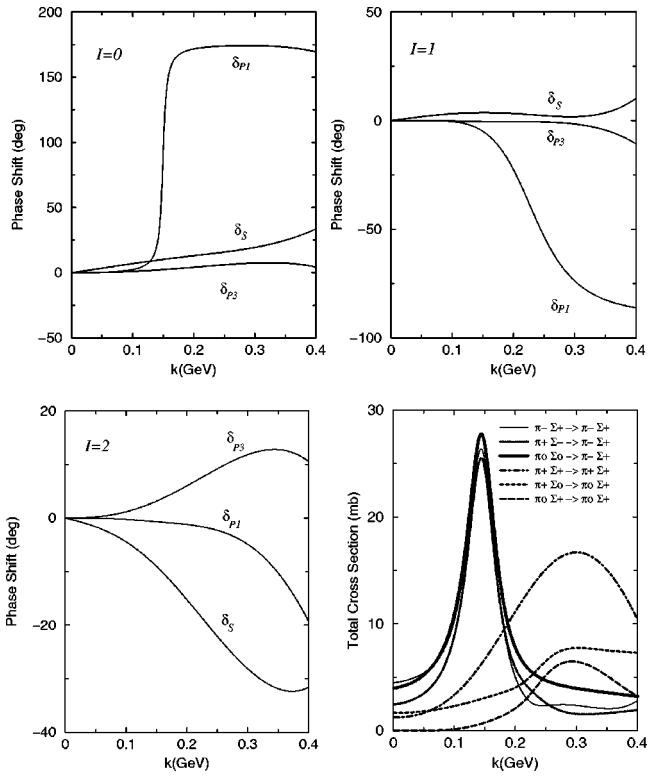

FIG. 4. Phase shifts and the energy dependence of σ_t for $\pi\Sigma$ interactions.

$$A_\rho = -\frac{g_0^2}{m_\rho^2}(\mu_{\Sigma^0}-\mu_{\Sigma^-})\nu\frac{1-t/4m_\rho^2}{1-t/m_\rho^2},$$

$$B_\rho = \frac{g_0^2}{m_\rho^2}(1+\mu_{\Sigma^0}-\mu_{\Sigma^-})\frac{1-t/4m_\rho^2}{1-t/m_\rho^2}. \tag{27}$$

Finally, the σ term has been parametrized in the same way as for $\pi\Lambda$, by using Eqs. (11), with the same parameters. In addition to the parameters used in the $\pi\Lambda$ case, we use here $m_{\Lambda^*}=1.406$ GeV , $m_\rho=0.769$ GeV, $\mu_{\Sigma^0}=0.649$, $\mu_{\Sigma^-}=-0.16$ and $g_{\Sigma\pi\Sigma}=6.7$ [27]. The coupling constant $g_{\Sigma\pi\Lambda^*}$ is not known, but we can proceed in the same way as we have done before, comparing the calculated amplitudes with the Breit-Wigner expression. The best fit is obtained with $g_{\Sigma\pi\Lambda^*}=8.74\ \text{GeV}^{-1}$.

We show in Fig. 4 the phase shifts calculated as explained above. Also shown is the energy dependence of the cross section σ_t for each channel described below.

Using the isospin formalism we calculate the elastic, as well as the charge exchange, amplitudes as

$$\langle\pi^+\Sigma^+|T|\pi^+\Sigma^+\rangle=\langle\pi^-\Sigma^-|T|\pi^-\Sigma^-\rangle=T_2,$$

$$\langle\pi^+\Sigma^0|T|\pi^+\Sigma^0\rangle=\langle\pi^-\Sigma^0|T|\pi^-\Sigma^0\rangle=\langle\pi^0\Sigma^+|T|\pi^0\Sigma^+\rangle$$
$$=\langle\pi^0\Sigma^-|T|\pi^0\Sigma^-\rangle=\frac{T_2}{2}+\frac{T_1}{2},$$

$$\langle\pi^0\Sigma^0|T|\pi^0\Sigma^0\rangle=\frac{2T_2}{3}+\frac{T_0}{3},$$

$$\langle\pi^+\Sigma^-|T|\pi^+\Sigma^-\rangle=\langle\pi^-\Sigma^+|T|\pi^-\Sigma^+\rangle=\frac{T_2}{6}+\frac{T_1}{2}+\frac{T_0}{3},$$

$$\langle\pi^-\Sigma^+|T|\pi^+\Sigma^-\rangle=\langle\pi^+\Sigma^-|T|\pi^-\Sigma^+\rangle=\frac{T_2}{6}-\frac{T_1}{2}+\frac{T_0}{3},$$

$$\langle\pi^+\Sigma^0|T|\pi^0\Sigma^+\rangle=\langle\pi^-\Sigma^0|T|\pi^0\Sigma^-\rangle$$
$$=\langle\pi^0\Sigma^+|T|\pi^+\Sigma^0\rangle$$
$$=\langle\pi^0\Sigma^-|T|\pi^-\Sigma^0\rangle=\frac{T_2}{2}-\frac{T_1}{2},$$

$$\langle\pi^+\Sigma^-|T|\pi^0\Sigma^0\rangle=\langle\pi^-\Sigma^+|T|\pi^0\Sigma^0\rangle$$
$$=\langle\pi^0\Sigma^0|T|\pi^+\Sigma^-\rangle$$
$$=\langle\pi^0\Sigma^0|T|\pi^-\Sigma^+\rangle=\frac{T_2}{3}-\frac{T_0}{3}. \tag{28}$$

With these amplitudes, we can calculate σ_t, $d\sigma/d\Omega$ and P as functions of k and $x=\cos\theta$ for each channel. The results for Σ^+ in the final state are shown in Figs. 4–6.

We can see in Fig. 4 that, although the first resonance is important in $\pi\Sigma$ interactions, it is not as much as in the π^+p or $\pi\Lambda$ scatterings. The peak in the $\Lambda^*(1405)$-mass region is not so high (less than 30 mb) and it appears in the $I=0$ state ($\pi^-\Sigma^+$). We remark that the other reactions ($I=1$ and especially $I=2$) have comparable total cross sections.

Before passing to the next section, it is worthwhile making the following remarks. Even in the tree-level calculation and in the low-energy ($k\lesssim 0.4$ GeV) region that we are considering here, there could occur the exchange reactions $\pi\Lambda\rightleftharpoons\pi\Sigma$. The possible diagrams for these are similar to Fig. 1(b) and Figs. 3(b) and 3(e), with one of Λ (Σ) replaced by Σ (Λ). However, the contributions of these reactions are small compared with the elastic ones we examined in this paper. First, as mentioned before and as can be seen in Figs. 2 and 4, the direct resonances dominate over all the other processes, which appear as corrections to the former. They do not change the cross sections much, however are necessary to produce polarization. Now, $\pi\Sigma\to\pi\Lambda$, which is given by the Σ^* term together with ρ exchange one, is much smaller than $\pi\Lambda\to\pi\Lambda$, because the branching ratio of Σ^* decay is $(\Sigma^*\to\pi\Sigma)/(\Sigma^*\to\pi\Lambda)\sim 0.16$ [25]. As for $\pi\Lambda\to\pi\Sigma$ compared with $\pi\Sigma\to\pi\Sigma$, as mentioned above first we have $\sigma(\pi\Lambda\to\pi\Sigma)/\sigma(\pi\Lambda\to\pi\Lambda)\sim 0.16$ for each possible channel. Now, from Figs. 2 and 4, each $\pi\Lambda\to\pi\Lambda$ channel, compared with the sum of the three prominent $\pi\Sigma\to\pi\Sigma$ channels, gives $\sigma(\pi\Lambda\to\pi\Lambda)/\Sigma\sigma(\pi\Sigma\to\pi\Sigma)\sim 0.60$ on the average in the resonance region. So, we estimate that the overall $\pi\Lambda\to\pi\Sigma$ contribution is less than 20% of $\pi\Sigma\to\pi\Sigma$ examined here.

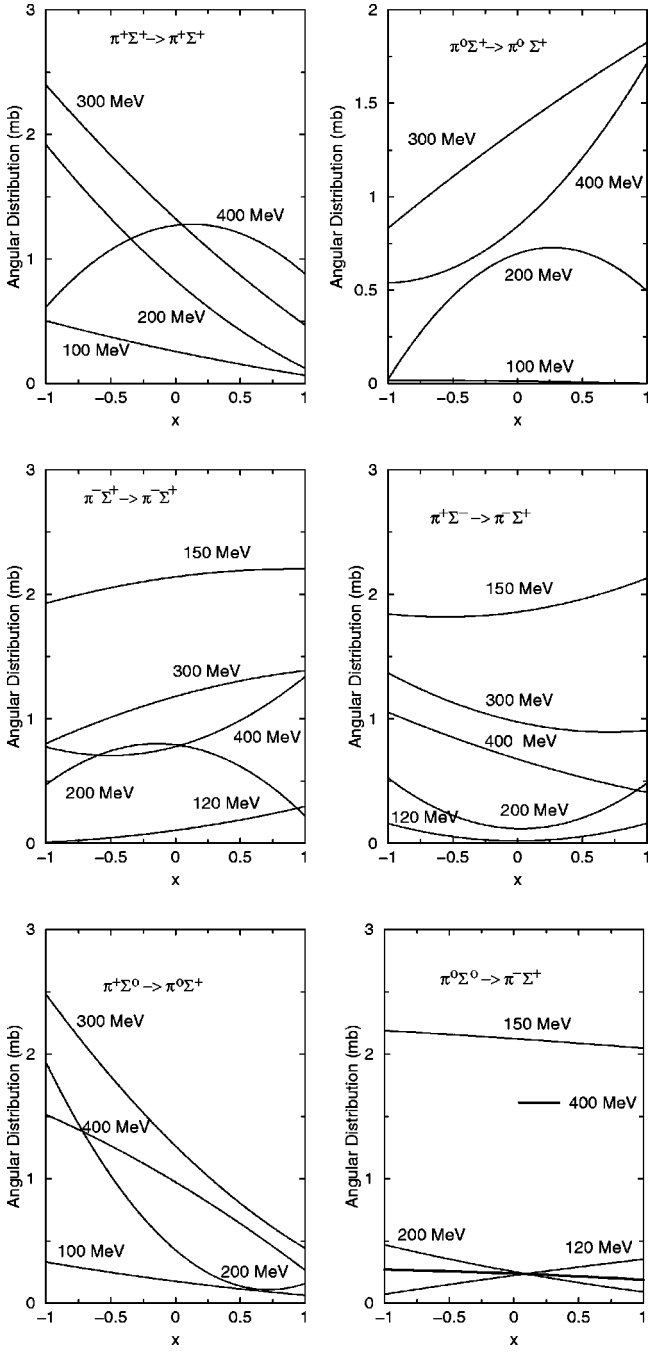

FIG. 5. Angular distributions of Σ^+.

V. $\pi\Xi$ INTERACTION

This case is very similar to the πN scattering, because Ξ has isospin 1/2 (as the nucleon) and the main difference is that the resonance of interest $\Xi^*(1533)$ has isospin $I=1/2$ [instead of $I=3/2$ as $\Delta(1232)$]. Then, the scattering amplitude $T^{ba}_{\pi\Xi}$ has the general form

$$T^{ba}_{\pi\Xi}=\overline{u}(\vec{p}\,')\left\{\left[A^+ + \frac{(\not{k}+\not{k}')}{2}B^+\right]\delta_{ba} + \left[A^- + \frac{(\not{k}+\not{k}')}{2}B^-\right] i\epsilon_{bac}\tau^c\right\} u(\vec{p}). \qquad (29)$$

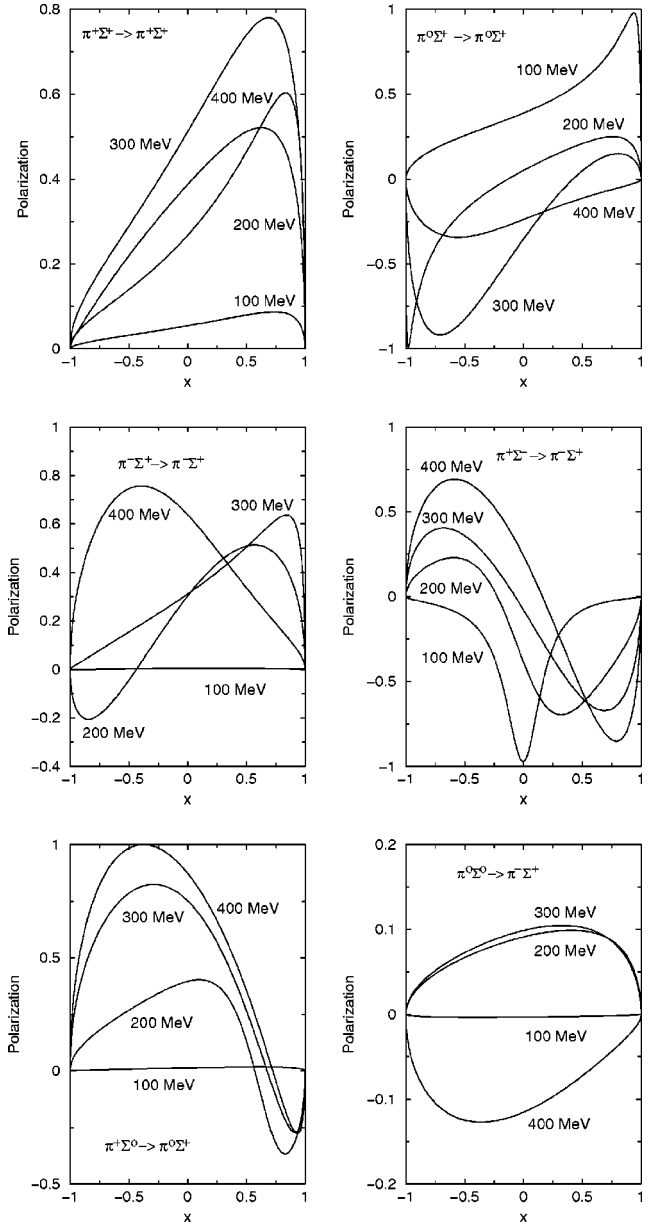

FIG. 6. Polarization of Σ^+.

The contributing diagrams are in Fig. 7 and the Lagrangians are almost the same as in the case of πN scattering, Eqs. (1)–(4), where we must replace the N field by Ξ field, and $\Delta(1232)$ by $\Xi^*(1533)$. The latter implies a substitution of the isospin matrix $\vec{M}$ by $\vec{\tau}$. Consequently, $A^{\pm}_{\Xi^*}$ and $B^{\pm}_{\Xi^*}$ have different structures as compared with $A^{\pm}_{\Delta}$ and $B^{\pm}_{\Delta}$ of πN case, whereas all the other $A^{\pm}$ and $B^{\pm}$ remain the same, with appropriate parameter changes.

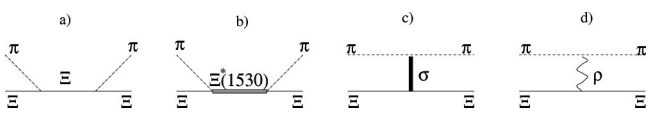

FIG. 7. Diagrams to $\pi\Xi$ interaction.

So, by computing the Feynman diagram in Fig. 7(a), we obtain

$$A^+_\Xi = \frac{g^2_{\Xi\pi\Xi}}{m_\Xi},$$

$$A^-_\Xi = 0,$$

$$B^+_\Xi = \frac{g^2_{\Xi\pi\Xi}}{m_\Xi}\frac{\nu}{\nu_0^2-\nu^2},$$

$$B^-_\Xi = -\frac{g^2_{\Xi\pi\Xi}}{2m^2_\Xi} - \frac{g^2_{\Xi\pi\Xi}}{m_\Xi}\frac{\nu_0}{\nu_0^2-\nu^2}. \tag{30}$$

The ρ exchange, Fig. 7(d), gives

$$A^+_\rho = B^+_\rho = 0,$$

$$A^-_\rho = -\frac{g_0^2}{m_\rho^2}(\mu_{\Xi^0}-\mu_{\Xi^-})\nu\frac{1-t/4m_\rho^2}{1-t/m_\rho^2},$$

$$B^-_\rho = \frac{g_0^2}{m_\rho^2}(1+\mu_{\Xi^0}-\mu_{\Xi^-})\frac{1-t/4m_\rho^2}{1-t/m_\rho^2}. \tag{31}$$

The contributions from Fig. 7(b) with intermediate $\Xi^*(1533)$ are

$$A^+_{\Xi^*} = \frac{g^2_{\Xi\pi\Xi^*}}{3m_\Xi}\left\{\frac{\nu_r}{\nu_r^2-\nu^2}\hat{A} - \frac{m^2_\Xi + m_\Xi m_{\Xi^*}}{m^2_{\Xi^*}} \times(2m^2_{\Xi^*} + m_\Xi m_{\Xi^*} - m^2_\Xi + 2m^2_\pi) + \frac{4m_\Xi}{m^2_{\Xi^*}}[(m_\Xi + m_{\Xi^*})Z + (2m_{\Xi^*}+m_\Xi)Z^2]k\cdot k'\right\},$$

$$A^-_{\Xi^*} = \frac{g^2_{\Xi\pi\Xi^*}}{3m_\Xi}\left\{\frac{\nu}{\nu_r^2-\nu^2}\hat{A} + \frac{8m^2_\Xi\nu}{m^2_{\Xi^*}} \times[(m_\Xi + m_{\Xi^*})Z + (2m_{\Xi^*}+m_\Xi)Z^2]\right\},$$

$$B^+_{\Xi^*} = \frac{g^2_{\Xi\pi\Xi^*}}{3m_\Xi}\left\{\frac{\nu}{\nu_r^2-\nu^2}\hat{B} - \frac{8m^2_\Xi\nu Z^2}{m^2_{\Xi^*}}\right\},$$

$$B^-_{\Xi^*} = \frac{g^2_{\Xi\pi\Xi^*}}{3m_\Xi}\left\{\frac{\nu_r}{\nu_r^2-\nu^2}\hat{B} - m_\Xi\frac{(m_\Xi+m_{\Xi^*})^2}{m^2_{\Xi^*}} - \frac{4m_\Xi Z^2}{m^2_{\Xi^*}}k\cdot k' - \frac{4m_\Xi}{m^2_{\Xi^*}}[(2m^2_\Xi + 2m_\Xi m_{\Xi^*} - 2m^2_\pi)Z + (2m^2_\Xi + 4m_\Xi m_{\Xi^*})Z^2]\right\}, \tag{32}$$

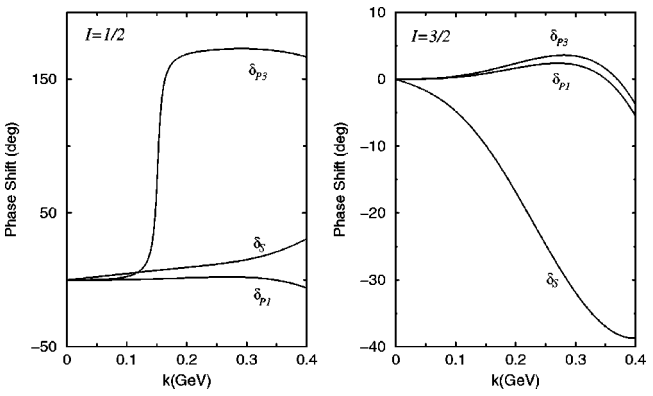

FIG. 8. Phase shifts for $\pi\Xi$ interaction.

where

$$\hat{A} = \frac{(m_{\Xi^*}+m_\Xi)^2 - m^2_\pi}{2m^2_{\Xi^*}}[2m^3_{\Xi^*} - 2m^3_\Xi - 2m_\Xi m^2_{\Xi^*} - 2m^2_\Xi m_{\Xi^*} + m^2_\pi(2m_\Xi - m_{\Xi^*})] + \frac{3}{2}(m_\Xi + m_{\Xi^*})t,$$

$$\hat{B} = \frac{1}{2m^2_{\Xi^*}}[(m^2_{\Xi^*} - m^2_\Xi)^2 - 2m^2_\pi(m_{\Xi^*}+m_\Xi)^2 + m^4_\pi] + \frac{3}{2}t. \tag{33}$$

The parameters used are $m_\Xi = 1.318$ GeV, $m_{\Xi^*} = 1.533$ GeV, $\mu_{\Xi^0} = -1.25$, $\mu_{\Xi^-} = 0.349$ and $g_{\Xi\pi\Xi} = 4$. As in the previous cases, we determined the $\Xi\pi\Xi^*$ coupling constant by using the Breit-Wigner formula and got the value $g_{\Xi\pi\Xi^*} = 4.54\ \text{GeV}^{-1}$. We display in Fig. 8 the calculated phase shifts to the isospin 1/2 and 3/2 states.

We can now obtain the matrix elements for each elastic and charge-exchange channel as

$$\langle\pi^+\Xi^0|T|\pi^+\Xi^0\rangle = \langle\pi^-\Xi^-|T|\pi^-\Xi^-\rangle = T_{3/2},$$

$$\langle\pi^+\Xi^-|T|\pi^+\Xi^-\rangle = \langle\pi^-\Xi^0|T|\pi^-\Xi^0\rangle = \frac{1}{3}T_{3/2} + \frac{2}{3}T_{1/2},$$

$$\langle\pi^0\Xi^-|T|\pi^0\Xi^-\rangle = \langle\pi^0\Xi^0|T|\pi^0\Xi^0\rangle = \frac{2}{3}T_{3/2} + \frac{1}{3}T_{1/2},$$

$$\langle\pi^0\Xi^-|T|\pi^-\Xi^0\rangle = \langle\pi^+\Xi^-|T|\pi^0\Xi^0\rangle = \frac{\sqrt{2}}{3}T_{3/2} - \frac{\sqrt{2}}{3}T_{1/2},$$

$$\langle\pi^-\Xi^0|T|\pi^0\Xi^-\rangle = \langle\pi^-\Xi^+|T|\pi^0\Xi^0\rangle = \frac{\sqrt{2}}{3}T_{3/2} - \frac{\sqrt{2}}{3}T_{1/2}. \tag{34}$$

We show, in Fig. 9, the integrated cross sections, with Ξ^- in the final state, obtained with these matrix elements. We can see that in this case the $\Xi(1533)$ resonance contribution is very important and it dominates three of the reactions. Figure 10 presents the angular distributions and polarizations for the same reactions.

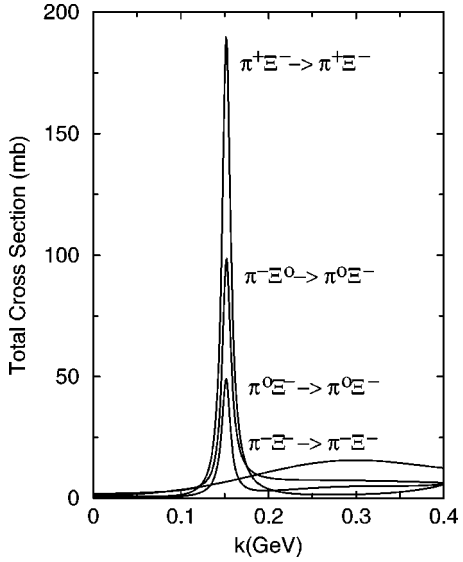

FIG. 9. Total cross sections for $\pi\Xi$ interaction.

VI. DISCUSSION OF THE RESULTS

In the preceding sections, by making a close analogy with the well established πN case, we have calculated the *S*- and *P*-wave phase shifts for $\pi\Lambda$, $\pi\Sigma$ and $\pi\Xi$ interactions, then obtained both the integrated and differential cross sections and polarizations for all the elastic and charge-exchange processes. Let us now discuss these results in connection with the two applications we mentioned in the Introduction.

The first application refers to the study of the CP violation. One of the ways to verify this violation is to observe the hyperon weak decays, $\Lambda\rightarrow\pi N$, $\Sigma\rightarrow\pi N$, $\Xi\rightarrow\pi\Lambda$, and $\Omega\rightarrow\pi\Xi$. In such a study, we need an independent estimate of the strong-interaction phase shifts in the final state.

For Λ and Σ decays, a large amount of data are available on the strong interaction phase shifts, since πN scatterings are very well studied. In the Ξ decay, there are some estimates of the *S*- and $P1$-wave phase shifts for $\pi\Lambda$ system. However, the reported results conflict with each other. Whereas the authors of [3] give $\delta_S=-18.7°$ and $\delta_{P1}=-2.7°$, in [5], they tell that $\delta_S=1.2°$ and $\delta_{P1}=-1.7°$ and, as for Ref. [4], δ_S is between $-1.3°$ and $0.1°$ and δ_{P1} between $-0.4°$ and $-3.0°$. In our calculation, with the σ term included, we obtained $\delta_{P1}=-0.36°$ and $\delta_S=-4.69°$ at the Λ-mass value, which gives $\delta_S-\delta_{P1}\sim-4.3°$, which is still small. One should remark that to really fit the phase shifts in πN scattering, especially δ_S, it is necessary to include other contributions as the diffractive [16] or the contact [21] terms with correct parameters. So it is possible that some correction is needed in the results we have obtained here.

In this paper, we have also calculated the $\pi\Xi$ phase shifts. So, it is possible to get some information about the CP violation in the $\Omega\rightarrow\pi\Xi$ decay, too. Ω has $J^p=\frac{3}{2}^+$, so the phase shifts we need are δ^I_{P3} and δ^I_{D3}. Calculating the asymmetry parameter A in the same way as in [5], the approximate expression reads

$$A=-\tan(\delta^{1/2}_{P3}-\delta^{1/2}_{D3})\tan(\phi^{1/2}_{P3}-\phi^{1/2}_{D3})$$
$$\sim-\tan(\delta^{1/2}_{P3})\tan(\phi^{1/2}_{P3}-\phi^{1/2}_{D3}). \quad (35)$$

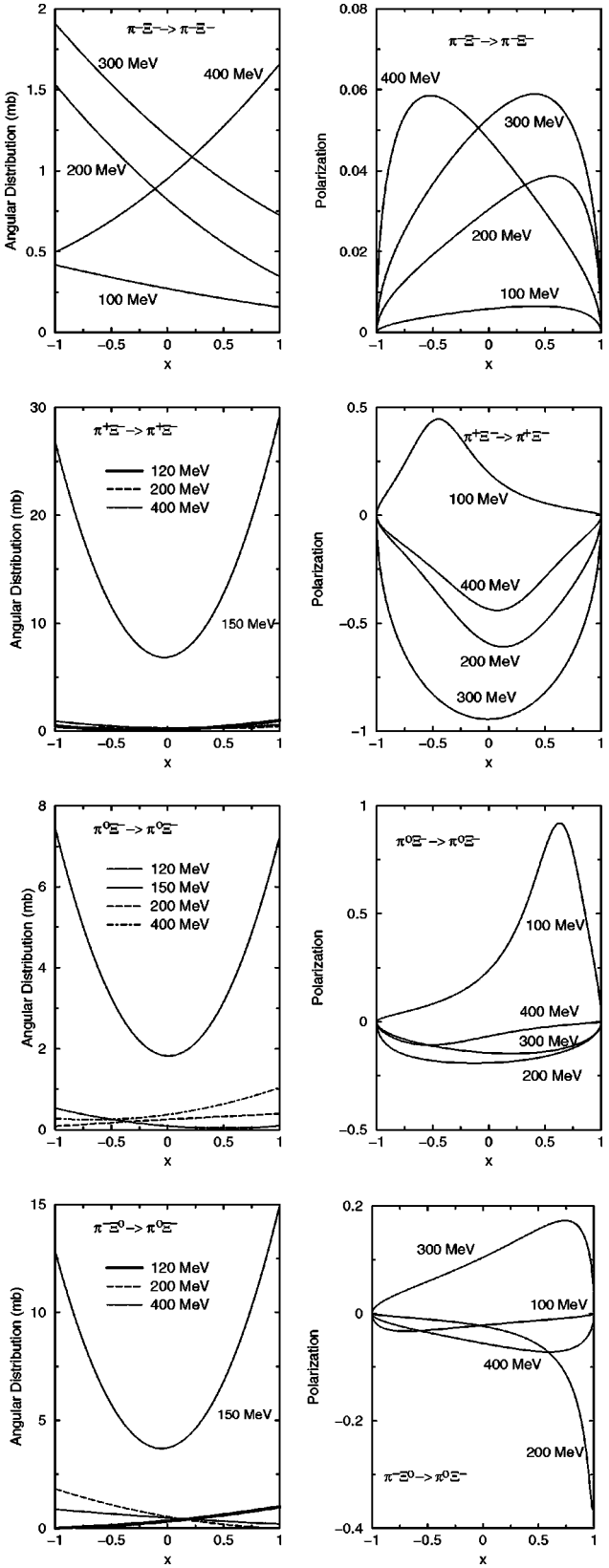

FIG. 10. $d\sigma/d\Omega$ and polarizations for Ξ^- production.

At the Ω mass value, $\delta^{1/2}_{D3}=0.21°$ (computed with the same diagrams used in Sec. V) and $\delta^{1/2}_{P3}=173.04°=180°-6.96°$. So the strong interaction effect in the asymmetry parameter will appear as $\tan(-7.17°)$, which is value close

to that obtained in the Ξ decay. So we do not expect that, in the study of CP violation in hyperon weak decays, $\Omega \to \pi\Xi$ is very useful.

The other application we mentioned in the Introduction, and which was the main motivation of this work, is the inclusive (anti-) hyperon polarization in high-energy collisions. As explained there, the antihyperon polarization cannot be understood in terms of the usual models [9–13], because all of them are based on the leading-particle effect and an antihyperon cannot be a leading particle. In [15] it has been proposed that antihyperons are polarized when interacting with the surrounding particles, which are predominantly pions, that make the environment where they are produced. So the antihyperon polarization would appear as an average effect of the low energy $\pi\overline{Y}$ interaction. It is clear that, generally speaking, such an average procedure washes out any existent asymmetry, so that no polarization would appear as a consequence. This is true if we look at the central region of the collision. However, the polarization data are obtained in very forward directions where the asymmetry could be preserved. Such calculations will be reported elsewhere [28], but just observing the results of the preceding sections we can draw some conclusions. The Λ polarization, as seen in Fig. 2, is positive below 100 MeV and then changes sign, so we expect that, on averaging, the large part will be canceled out, implying the polarization of $\overline{\Lambda} \sim 0$. As seen in Figs. 9 and 10, the Ξ^- polarization is negative and very large in the channels where the cross section is large, whereas the Σ^- polarization is positive in most of the cases, Fig. 6. As we can see, the hyperon polarization is different in each case, and seems to be consistent with the experimental data for the antihyperons [7,8]. We remark that the polarization sign changes under charge conjugation.

ACKNOWLEDGMENTS

We would like to thank M.R. Robilotta for discussions about the hadron interactions and comments on the manuscript. This work was partially supported by CNPq and FAPESP (Contract Nos. 98/02249-4 and 00/04422-7).

APPENDIX: BASIC FORMALISM

In this paper p and p' are the initial and final hyperon four-momenta, k and k' are the initial and final pion four-momenta, so the Mandelstam variables are

$$s=(p+k)^2=(p'+k')^2, \tag{A1}$$

$$t=(p-p')^2=(k-k')^2, \tag{A2}$$

$$u=(p'-k)^2=(p-k')^2. \tag{A3}$$

With these variables, we can define

$$\nu=\frac{s-u}{4m}, \tag{A4}$$

$$\nu_0=\frac{2m_\pi^2-t}{4m}, \tag{A5}$$

$$\nu_r=\frac{m_r^2-m^2-k\cdot k'}{2m}, \tag{A6}$$

where m, m_r, and m_π are, respectively, the hyperon mass, the resonance mass, and the pion mass. The scattering amplitude for an isospin I state is

$$T_I=\overline{u}(\vec{p}')\left\{\left[A^I+\frac{(\not{k}+\not{k}')}{2}B^I\right]\right\}u(\vec{p}), \tag{A7}$$

where A_I and B_I are calculated using the Feynman diagrams. So the scattering matrix is

$$M_I^{ba}=\frac{T_I^{ba}}{8\pi\sqrt{s}}=f_I(\theta)+\vec{\sigma}\cdot\hat{n}g_I(\theta)=f_1^I+\frac{(\vec{\sigma}\cdot\vec{k}')(\vec{\sigma}\cdot\vec{k})}{kk'}f_2^I, \tag{A8}$$

with

$$f_1^I(\theta)=\frac{(E+m)}{8\pi\sqrt{s}}[A_I+(\sqrt{s}-m)B_I], \tag{A9}$$

$$f_2^I(\theta)=\frac{(E-m)}{8\pi\sqrt{s}}[-A_I+(\sqrt{s}+m)B_I], \tag{A10}$$

where E is the hyperon energy. The partial-wave decomposition is done with

$$a_{l\pm}=\frac{1}{2}\int_{-1}^{1}[P_l(x)f_1(x)+P_{l\pm1}(x)f_2(x)]dx. \tag{A11}$$

In our calculation (tree level) $a_{l\pm}$ is real. With the unitarization, as explained in Sec. III, we obtain

$$a_{l\pm}^U=\frac{1}{2ik}[e^{2i\delta_{l\pm}}-1]=\frac{e^{i\delta_{l\pm}}}{k}\mathrm{sen}(\delta_{l\pm})\to a_{l\pm}. \tag{A12}$$

These complex amplitudes are used to calculate

$$f(\theta)=\sum_{l=0}^{\infty}[(l+1)a_{l+}+la_{l-}]P_l(x), \tag{A13}$$

$$g(\theta)=i\sum_{l=1}^{\infty}[a_{l+}-a_{l-}]P_l^{(1)}(x). \tag{A14}$$

We have, then, in the center-of-mass frame,

$$\frac{d\sigma}{d\Omega}=|f|^2+|g|^2, \tag{A15}$$

$$\vec{P}=-2\frac{\mathrm{Im}(f^*g)}{|f|^2+|g|^2}\hat{n}, \tag{A16}$$

$$\sigma_t=4\pi\sum_l[(l+1)|a_{l+}|^2+l|a_{l-}|^2]. \tag{A17}$$

[1] S. Okubo, Phys. Rev. **109**, 984 (1958).
[2] A. Pais, Phys. Rev. Lett. **3**, 242 (1959).
[3] R. Nath and A. Kumar, Nuovo Cimento **36**, 669 (1965).
[4] A. Datta, P. O'Donnell, and S. Pakvasa, hep-ph/9806374.
[5] A. N. Kammal, Phys. Rev. D **58**, 077501 (1998).
[6] G. Bunce *et al.*, Phys. Rev. Lett. **36**, 1113 (1976); K. Heller *et al.*, *ibid.* **41**, 607 (1978); R. Ramerika *et al.*, Phys. Rev. D **33**, 3172 (1986); C. Wilkinson *et al.*, Phys. Rev. Lett. **58**, 855 (1987).
[7] P. M. Ho *et al.*, Phys. Rev. D **44**, 3402 (1991).
[8] A. Morelos *et al.*, Phys. Rev. Lett. **71**, 2172 (1993).
[9] B. Andersson, G. Gustafson, and G. Ingelman, Phys. Lett. **85B**, 417 (1979).
[10] T. A. DeGrand and H. I. Miettinen, Phys. Rev. D **24**, 2419 (1981).
[11] J. Soffer and N. A. Törnqvist, Phys. Rev. Lett. **68**, 907 (1992).
[12] S. M. Troshin and N. E. Tyurin, Phys. Rev. D **55**, 1265 (1997).
[13] Y. Yamamoto, K. Kubo, and H. Toki, Prog. Theor. Phys. **98**, 95 (1997); K. Kubo, Y. Yamamoto, and H. Toki, *ibid.* **101**, 615 (1999); Y. Kitsukawa and K. Kubo, *ibid.* **103**, 1173 (2000).
[14] M. Anselmino, D. Boer, U. D'Alesio, and F. Murgia, Phys. Rev. D **63**, 054029 (2001).
[15] Y. Hama and T. Kodama, Phys. Rev. D **48**, 3116 (1993).
[16] M. G. Olsson and E. T. Osypowsky, Nucl. Phys. **B101**, 136 (1975).
[17] B. C. Pearce and B. K. Jennings, Nucl. Phys. **A528**, 655 (1991).
[18] D. Bonfinger and W. S. Woolcock, Nuovo Cimento A **104**, 1489 (1991).
[19] F. Gross and Y. Surya, Phys. Rev. C **47**, 703 (1993).
[20] P. F. A. Goudsmit, H. J. Leisi, E. Matsinos, B. L. Birbrair, and A. B. Gridnev, Nucl. Phys. **A575**, 673 (1994).
[21] P. J. Ellis and H. B. Tang, Phys. Rev. C **56**, 3363 (1997).
[22] H. T. Coelho, T. K. Das, and M. R. Robilotta, Phys. Rev. C **28**, 1812 (1983).
[23] A.M.M. de Menezes, Master thesis, University of São Paulo, 1985.
[24] M. L. Perl, *High Energy Hadron Physics* (Wiley-Interscience, New York, 1974).
[25] Particle Data Group, C. Caso *et al.*, Eur. Phys. J. C **3**, 1 (1998).
[26] B. R. Martin, Phys. Rev. **138**, B1136 (1965).
[27] H. Pilkuhn, *The Interaction of Hadrons* (North-Holland, Amsterdam, 1967).
[28] C. C. Barros, Jr. and Y. Hama (unpublished).